Zoological Studies **65:**55 (2026)

Genome-wide SNPs Reveal Long-term Genetic Divergence Despite Secondary Contact during Pleistocene Land Bridge Formation in *Kurixalus eiffingeri* (Amphibia: Rhacophoridae)

Ryo Kamimura[1,*], Shumei Sakihama[2], Chi-Shiun Wu[3], Yi-Huey Chen[3], Masafumi Matsui[4], Natsuhiko Yoshikawa[5], and Atsushi Tominaga[1,2,*]

[1]*Graduate School of Engineering and Science, University of the Ryukyus, Senbaru 1, Nishihara, Okinawa 903-0213, Japan. *Correspondence: E-mail: r.kamimura.kurixalus@gmail.com (Kamimura); tominaga@cs.u-ryukyu.ac.jp (Tominaga)*

[2]*Faculty of Education, University of the Ryukyus, Senbaru 1, Nishihara, Okinawa 903-0213, Japan. E-mail: 7515gjmwtp.adptwgjmdmw@ezweb.ne.jp (Sakihama)*

[3]*Department of Life Science, Chinese Culture University, 55, Hwa-Kang Rd., Yang-Ming-Shan, Taipei, Taiwan. E-mail: buergeria@gmail.com (Wu); yihueyc@gmail.com (Chen)*

[4]*Graduate School of Human and Environmental Studies, Kyoto University, Yoshida Nihonmatsu-cho, Sakyo, Kyoto 606-8501, Japan. E-mail: fumi@zoo.zool.kyoto-u.ac.jp (Matsui)*

[5]*Department of Zoology, National Museum of Nature and Science, Tokyo 4-1-1 Amakubo, Tsukuba, Ibaraki 305-0005 Japan. E-mail: onychodactylus@gmail.com (Yoshikawa)*

(Received 26 February 2026 / Accepted 18 August 2026 / Published -- 2026)

Communicated by Si-Min Lin

Sea-level fluctuations during Pleistocene glacial cycles repeatedly connected and isolated islands in the Ryukyu Archipelago, but the extent to which these events promoted gene flow remains unclear for many terrestrial taxa. The tree frog *Kurixalus eiffingeri* occurs on Ishigaki and Iriomote Islands in the Yaeyama group and in Taiwan, and previous mitochondrial DNA analyses revealed deep divergence among populations despite their geographic proximity. To test whether nuclear genomic data supports this pattern, we analysed genome-wide SNPs generated by MIG-seq. Phylogenetic

reconstruction, STRUCTURE analysis, and principal component analysis consistently identified four major genetic clusters corresponding to Ishigaki, Iriomote, northern Taiwan, and central Taiwan, with the Ishigaki and Iriomote clusters forming the Ryukyu clade. Despite the clear genetic distinctiveness between the Ishigaki and Iriomote clusters, model-based demographic inference using dadi identified the secondary contact model as the best-fitting scenario, suggesting a history of long-term genetic divergence followed by secondary contact during Pleistocene land bridge formation. This pattern may reflect either limited suitable habitat on the Pleistocene land bridge, which restricted gene flow, or partial reproductive isolation between the two clusters, with limited gene flow across a hybrid zone on the land bridge.

Keywords: Continental islands, Genome-wide SNPs; *Kurixalus*, Rhacophoridae, Ryukyu Archipelago, Secondary contact

Citation: Kamimura R, Sakihama S, Wu CS, Chen YH, Matsui M, Yoshikawa N, Tominaga A. 2026. Genome-wide SNPs reveal long-term genetic divergence despite secondary contact during pleistocene land bridge formation in *Kurixalus eiffingeri* (Amphibia: Rhacophoridae). Zool Stud **65:**55.

BACKGROUND

Sea-level fluctuations associated with glacial and interglacial periods have repeatedly connected and isolated continental islands from adjacent landmasses, leading to cycles of geographic isolation (Lomolino et al. 2006). This isolation is widely regarded as a major driver of species diversification on islands (de Queiroz 2005) and represents a distinctive evolutionary process shaping insular biota. In addition to these geohistorical events, the traits of island organisms are influenced by a range of biotic and abiotic factors, including island size, environmental conditions, and species richness (MacArthur and Wilson 1963; Wilson and MacArthur 1967) which

can drive the emergence of endemic species through adaptive radiation and facilitate allele fixation via genetic drift in small populations (Witt and Maliakal-Witt 2007).

For decades, much debate has focused on whether terrestrial faunas on islands originated via vicariant events, such as colonisation via land bridge followed by isolation, or through long-distance overseas dispersal (de Queiroz 2005; Yoder and Nowak 2006; Stelbrink et al. 2012). Recent advances in molecular phylogenetics have made it possible to estimate divergence times and phylogenetic relationships between island taxa and their continental relatives, allowing historical biogeographical hypotheses to be tested against geological data (de Queiroz 2005).

Mitochondrial DNA (mtDNA), widely utilized in taxonomy and molecular phylogenetic studies, possesses characteristics such as maternal inheritance, haploidy, and a high mutation rate, making it effective for reconstructing both intraspecific and interspecific evolutionary histories. However, mtDNA has well-documented limitations in resolving complex patterns of hybridisation and introgression (Toews and Brelsford 2012). In recent years, the widespread adoption of next-generation sequencing technologies has enabled genome-wide analyses based on nuclear DNA (nuDNA), providing more comprehensive and higher-resolution phylogenetic inferences (Marshall et al. 2021). Because nuDNA is inherited biparentally and encompasses information from numerous loci, it allows for more accurate assessments of historical gene flow and admixture between populations than mtDNA, which represents only a single locus. Consequently, discordance between mtDNA and nuDNA phylogenies (Marshall et al. 2021; Tominaga et al. 2022) as well as evidence of introgression between divergent clusters or closely related species have been frequently reported across various animal taxa (Dufresnes et al. 2020; Ge et al. 2022; Horoiwa et al. 2021; Kato et al. 2024; Kvie et al. 2013; Shimada et al. 2022; Zhang et al. 2019).

The Yaeyama group of islands, located in the southwestern part of the Ryukyu Archipelago, were historically connected to Taiwan and the Eurasian continent (Kizaki and Oshiro 1977 1980; Ujiie 1986; Kimura 1996), and these Islands retain a biota with strong affinities to those regions (Ota 1998; Motokawa 2000). Meanwhile, the Sekisei Lagoon, which is a shallow body of water (only several metres deep), separating Ishigaki and Iriomote Islands in the Yaeyama group of

islands has been repeatedly affected by sea-level changes during glacial cycles (Lambeck and Chappell 2001; Bintanja et al. 2005; Bintanja and Roderik 2008; Fernández-Palacios et al. 2016), hich have caused multiple episodes of land connection and separation between these islands (Kizaki and Oshiro 1977 1980; Ujiie 1986; Kimura 1996; Ota 1998; Motokawa 2000). Consequently, low levels of genetic divergence between populations on each island have been reported for many animal taxa (Matsui et al. 2005; Brandley et al. 2011; Tominaga et al. 2015; Kaito and Toda 2016; Su et al. 2016). In contrast, species with narrow habitat ranges restricted to mountain streams, such as *Odorrana utsunomiyaorum* and *Euphaea yayeyamana*, exhibit significant genetic divergence between island populations (Matsui et al. 2005; Kanke et al. 2021). *Kurixalus eiffingeri* which is distributed across Ishigaki Island, Iriomote Island, and Taiwan, occupies a broad range within each island. Nevertheless, phylogenetic analyses based on mtDNA have revealed that populations from each island formed monophyletic clades, with substantial genetic divergence despite their broad geographic distribution (Kamimura et al. 2025).

In the present study, we conducted genome-wide population genetic analyses using single nucleotide polymorphism (SNP) data to evaluate whether the phylogenetic structure inferred from mtDNA is also supported by nuclear DNA. Our goal was to achieve a higher resolution understanding of the evolutionary history and genetic differentiation between Ishigaki and Iriomote populations.

MATERIALS AND METHODS

Sampling

A total of 46 individuals of *Kurixalus eiffingeri* from seven sites on Ishigaki Island, 34 individuals from four sites on Iriomote Island, and six individuals from two sites in Taiwan were analysed in this study, together with eight individuals of the congeneric species *K. idiootocus* from

five sites in Taiwan (Fig. 1, Table 1). Thigh muscles and liver were collected from each specimen and frozen in 99% ethanol for DNA analysis. The other body parts were fixed in 10% formalin, replaced with 70% ethanol, and preserved as voucher specimens. These procedures were approved by the Animal Experiment Committee of the University of the Ryukyus and were conducted in accordance with the experimental guidelines (approval number: A2021054). To extract DNA, muscle tissues of each individual kept in 99% ethanol were shredded in 660 µL of 1× STE Buffer and 60 µL of 10% SDS solution. To these solutions, 10 µL proteinase K (23 ng/µL) was added and incubated overnight at 50°C in an incubator to degrade the proteins. DNA was purified from these solutions using protein precipitation solution (Promega, Madison, WI, USA). Finally, the extracted DNA was dissolved in approximately 100 µL of 1×TE Buffer and refrigerated.

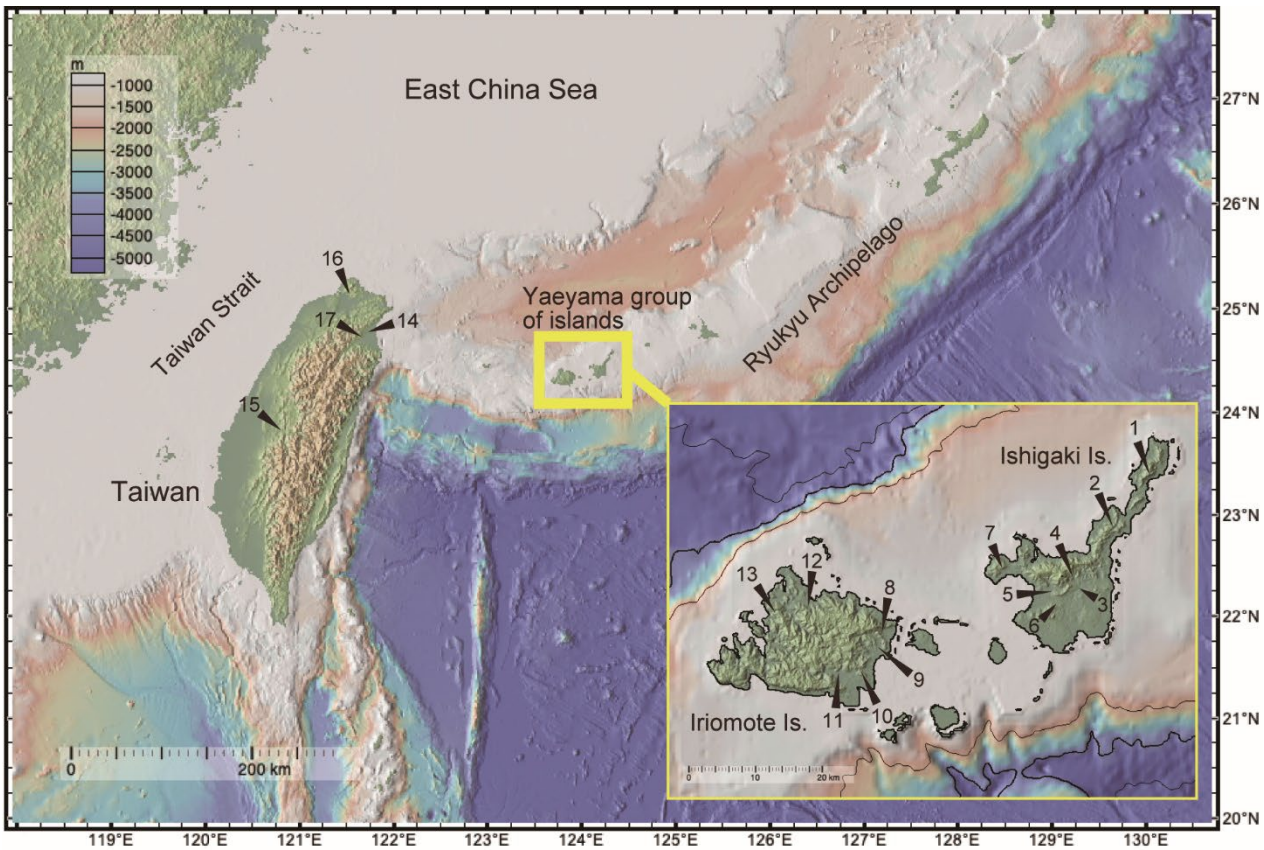

Fig 1. Maps showing the sampling locations of *Kurixalus eiffingeri* and *K. idiootocus* included in this study. The numbers of the above sampling sites are listed in table 1. The map was prepared using GeoMapApp (Ryan et al. 2009; available at www.geomapapp.org; accessed 19 Aug. 2026).

Table 1. Species, sampling locations, and number of specimens used for genetic analyses

Species	Sampling location number	Locality	No. of examined specimens
K. eiffingeri	Ishigaki Island		
	1	Hirakubo	6
	2	Nosoko	5
	3	Ohama	3
	4	Hirae	17
	5	Tonoshiro	2
	6	Ishigaki	4
	7	Sakieda	9
	Iriomote Island		
	8	Takana	4
	9	Komi	5
	10	Haiminaka	1
	11	Haimi	8
	12	Uehara	1
	13	Iriomote	14
	Taiwan		
	14	Yilan	4
	15	Chiayi	2
K. idiootocus	16	Taipei	3
	17	Yilan	4

MIG-seq

SNP analysis was performed using multiplexed ISSR genotyping by sequencing (MIG-seq) with some modifications of the protocol of Suyama and Matsuki (2015) as below. To amplify thousands of short inter-simple sequence repeats (ISSRs) from genomic DNA, 30 ng/μL of template DNA was used for the first PCR. The first PCR was performed using eight pairs of forward and

reverse multiplex primers, Multiplex PCR Assay Kit v.2 (TaKaRa, Kusatsu, Shiga, Japan) and a total reaction volume of 7 μL. The thermal cycling condition consisted of an initial denaturation at 94°C for 1 minute, followed by 25 cycles of 94°C for 30 seconds, 38°C for 1 minute, 72°C for 1 min, with a final extension at 72°C for 10 minutes. As a modification of the protocol by Suyama & Matsuki (2015), the annealing temperature was changed from 48°C to 38°C to enhance DNA amplification. The first PCR product for each individual was diluted 40-fold with 0.5×TE. The second PCR was conducted using PrimeSTAR GXL DNA polymerase (TaKaRa, Kusatsu, Shiga, Japan) in a total reaction volume of 12 μL under the following conditions: one cycle of 94°C for 1 min, followed by 12 cycles of 98°C for 10 sec, 54°C for 15 seconds, and 68°C for 30 seconds. Then, 3 μL of each PCR product was combined in one tube and purified according to the protocol of the QIAquick PCR purification kit (Qiagen, Valencia, CA, USA). Fragments in the size range of 300-800 bp in the purified library were isolated using an automated gel extractor Blue Pippin and a 2% agarose gel cassette. The size-selected library was then purified again using the QIAquick PCR purification kit, and the quality of the library was confirmed on a 4200 Tape Station (Agilent Technologies, Santa Clara, CA, USA). The concentration of the purified final library was measured with a Qubit 4 Fluorimeter (Invitrogen, CA, USA) and diluted with pure water to 4 nM. The prepared library was diluted to approximately 6 pM according to Illumina's protocol and sequenced with the Illumina MiSeq Sequencer (Illumina, CA, USA) using the MiSeq Reagent Kit v3 (150-cycle, Illumina, CA, USA) using the Illumina MiSeq Sequencer (Illumina, CA, USA)..

Bioinformatics and de novo assembly

De novo assembly and subsequent analysis of the raw data obtained was performed using ipyrad 0.9.79 (Eaton and Overcast, 2020). The data type was specified as “ddrad” because MIG-seq targets short loci and produces relatively low per-locus sequencing depth, resulting in data characteristics broadly comparable to those of ddRAD sequencing. The sequence-clustering threshold was set to 0.90, and a minimum sequencing depth of four reads was required for genotype

calling. All other assembly parameters were left at their default settings. The concatenated sequences for each individual were output as a phylip file and used for phylogenetic analysis. SNP datasets for population genetic analyses were generated from the ipyrad snps.hdf5 database using the ipyrad-analysis toolkit. Insertion–deletion variants were excluded, and only biallelic SNPs were retained. Loci were retained when genotype data were available for at least 90% of all individuals and for at least 50% of individuals within each predefined population. The resulting filtered SNP datasets were used for STRUCTURE analysis and principal component analysis (PCA). The same assembly and SNP-filtering procedures were applied independently to three datasets: the complete *Kurixalus eiffingeri* dataset, an Ishigaki Island-only dataset, and an Iriomote Island-only dataset, to investigate population structure at multiple geographic scales.

Phylogenetic analysis based on SNPs data

Phylogenetic analysis based on sequence output as Phylip files was performed using the maximum likelihood method in RAxML-NG v. 1.0.2 (Kozlov et al. 2019). The evolutionary model used was GTR + G (Tavaré, 1986). The branching points were evaluated using 1000 booster trap iterations. The output files were illustrated in FigTree v1.4.4 (http://tree.bio.ed.ac.uk/software/figtree)

Population genetic analysis based on SNPs data

STRUCTURE analyses and PCA were performed on the *K. eiffingeri* dataset only, except for *K. idiootocus*. The analyses were performed using a Python script provided by the ipyrad-analysis toolkit (https://ipyrad.readthedocs.io/en/latest/API-analysis/index.html), and using the snps.hdf5 file output by ipyrad, a Python script provided by the ipyrad-analysis toolkit. In the “minmap” script, the data for each individual were assigned to the Ishigaki, Iriomote, and Taiwanese populations, and in mincov" the SNPs were assigned a minimum coverage per locus of

75% for all individuals and 50% for each population. PCA was performed using the Python packages pandas and toyplot (Shead 2014). The genetic admixture ratio of all individuals was calculated quantitatively based on a Bayesian clustering algorithm using STRUCTRE v.2.3.4 (Pritchard et al. 2000). Assuming an admixture model with correlated allele frequencies, the admixture ratio for each individual was calculated using the correlated allele frequency model (Evanno et al. 2005), with the number of clusters (K) set from 2 to 6. The first 5,000 data points were discarded as burn-in using Structure v.2.3.4 (Pritchard et al. 2000), followed by 100,000 Markov chain Monte Carlo (MCMC) runs. 5 MCMC runs were performed for each value of K. The difference between the clusters (ΔK) was calculated using an analytical platform. Five replications were performed for each, and the results were summarized using CLUMPP (Jakobsson & Rosenberg 2007) and depicted in a toyplot (Shead 2014). Similar analyses were performed independently on Ishigaki and Iriomote Island populations to determine the genetic structure within the islands.

Demographic inference

Demographic history between the Ishigaki and Iriomote clusters was inferred using dadi (Gutenkunst et al. 2009). A folded two-dimensional site frequency spectrum (2D-SFS) was generated from the filtered SNP dataset using easySFS (https://github.com/isaacovercast/easySFS), which randomly retained one SNP per locus to minimize the effects of linkage among markers. Projection sizes were set to 86 and 49 chromosomes for the Ishigaki and Iriomote clusters, respectively. Four demographic models were evaluated: Strict Isolation (SI), Isolation with Migration (IM), Ancient Migration (AM), and Secondary Contact (SC). The SI model assumes complete isolation following population divergence; the IM model assumes continuous migration after divergence; the AM model assumes migration immediately after divergence followed by complete isolation; and the SC model assumes an initial period of isolation followed by secondary contact (Fig. 2).

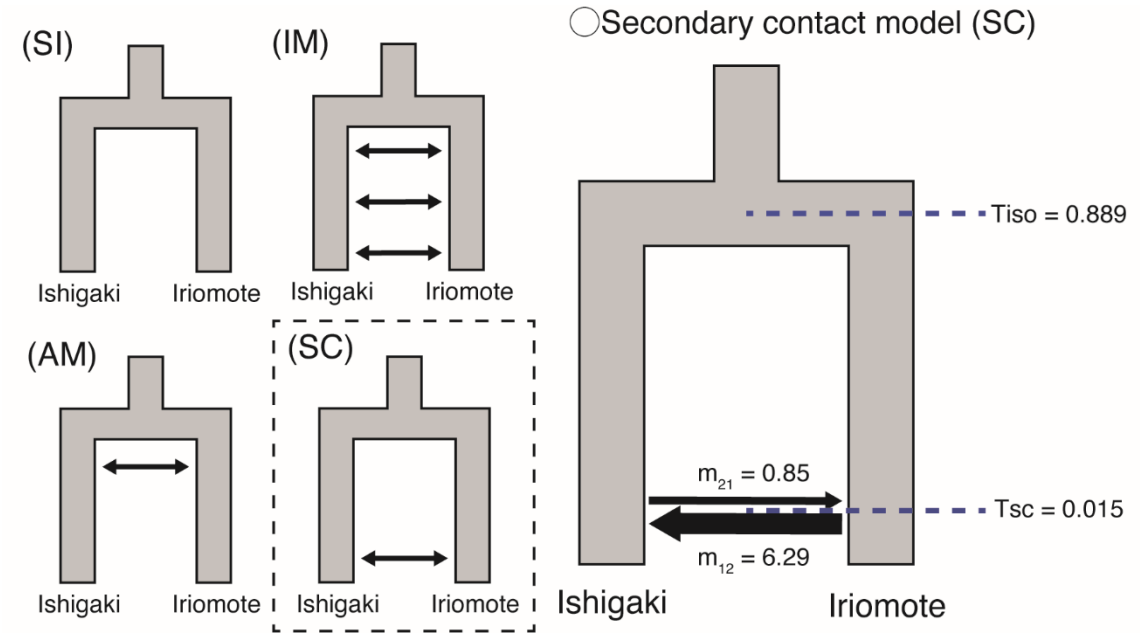

Fig. 2. Schematic illustration of all possible models for model selection in dadi. The Strict Isolation (SI) model assumes complete isolation after divergence. The Isolation with Migration (IM) model assumes continuous gene flow after divergence. The Ancient Migration (AM) model assumes that the two clusters experienced gene flow shortly after divergence and then became complete isolated. The Secondary Contact (SC) model assumes an initial period of divergence in isolation followed by recent secondary contact. The SC model provided the best fit to the data, suggesting that the Ishigaki and Iriomote clusters diverged, remained isolated for a period, and experienced recent secondary contact with limited gene flow.

Model parameters were optimized using "dadi. Inference.optimize_log_fmin." Initial parameter values were randomly perturbed for each optimization using "dadi.Misc.perturb_params" to reduce the likelihood of convergence on local optima. Each model was independently optimized 100 times, with a maximum of 300 iterations per optimization, and the replicate with the highest log-likelihood was retained for each model. Model support was evaluated using the Akaike Information Criterion (AIC).

Estimating absolute divergence times from dadi requires converting population-scaled time parameters into calendar time using an estimate of the ancestral effective population size (Ne), which depends on the population-scaled mutation parameter (θ) and the germline mutation rate (μ) (Tran et al. 2024). However, direct estimates of μ are currently unavailable for amphibians in general, precluding a reliable estimation of absolute divergence times from dadi data alone. Thus,

we used the previously estimated mtDNA divergence time between the Ishigaki and Iriomote clusters (1.41 MYA, 95% CI: 0.81–2.02; Kamimura et al. 2025) for external temporal calibration. Specifically, the mtDNA divergence time was assumed to correspond to the initial isolation phase (Tiso) and this calibration was used to convert the remaining demographic time parameters into approximate absolute ages.

\

RESULTS

Phylogenetic analysis based on SNPs data

The number of reads in the raw data by MIG-seq ranged from 13,326 to 175,489, and the number of detected SNPs was 22,654. The concatenated sequences contained 368,562 base pairs, including missing values. The phylogenetic tree estimated by the maximum likelihood method based on concatenated sequence data for each individual showed that the Ishigaki, Iriomote, northern Taiwan, and central Taiwan clusters were monophyletic (BS: 100%, 100%, 73%, and 100%, respectively) (Fig. 3), similar to the phylogenetic tree estimated from the mtDNA data. The Ishigaki and Iriomote clusters were combined into the Ryukyu clade (BS: 100%), and the Northern Taiwan and Ryukyu clusters were sister clades (BS: 73%).

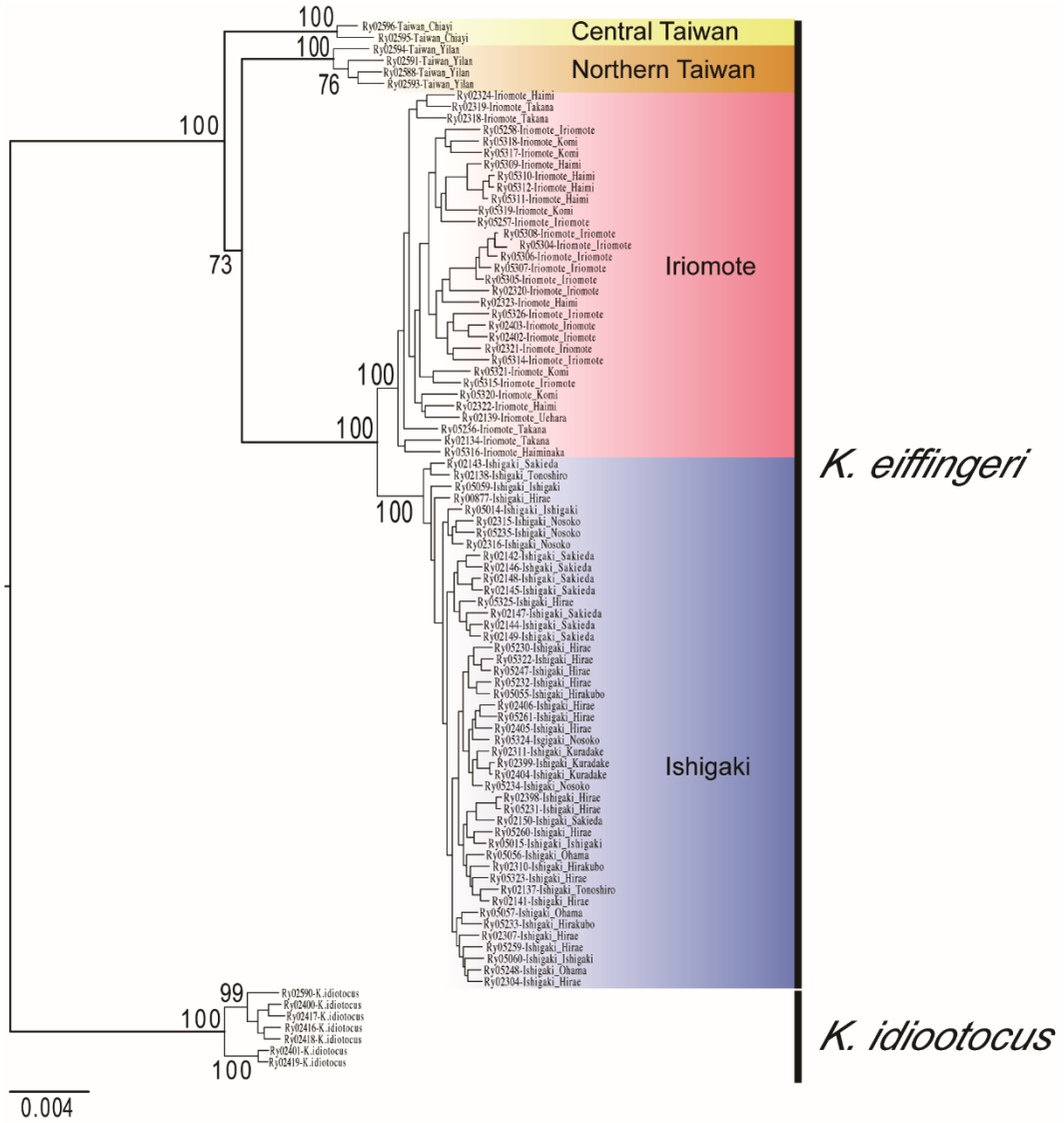

Fig. 3. Phylogenetic tree of *Kurixalus* spp. based on concatenated sequences (368,562) obtained by MIG-seq analyze estimated by maximum likelihood. Numbers denoted above nodes represent bootstrap supports (> 70%).

Population genetic analysis based on SNPs data

Filtering resulted in 878 SNPs, including 128 unlinked loci, which were used for population structure analyses of *Kurixalus eiffingeri*. STRUCTURE analyses were performed for *K* values ranging from 2 to 10. The *ΔK* method identified a primary signal at *K* = 3 (*ΔK* = 4.219; mean LnP(*K*) = -1916.1 ± 67.9; Fig. S1), which was considered the most parsimonious model for the full dataset. At *K* = 3, individuals were clearly assigned to three major genetic clusters corresponding to Ishigaki Island, Iriomote Island, and Taiwan (Fig. 4A). At *K* = 4, additional genetic substructure

became apparent within the Taiwanese samples, although the separation between the northern and central populations remained incomplete (Fig. S1). A clear subdivision into Northern and Central Taiwan clusters was first observed at $K = 5$ (Fig. 4B).

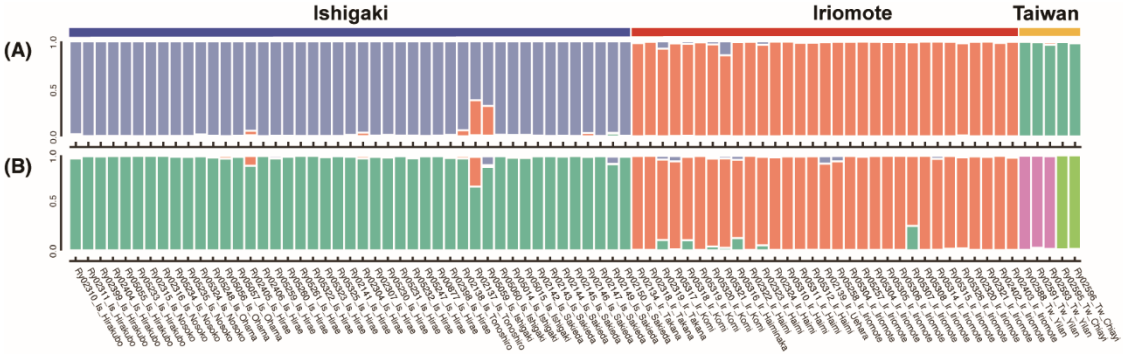

Fig. 4. Results of STRUCTURE analysis indicating admixture rate in each individual based on SNPs in Ishigaki Island, Iriomote Island, and Taiwan. (A) The samples were divided into three islands groups at the best number of clusters (K) = 3; (B) The samples were divided into four clusters (Ishigaki, Iriomote, the Central, and the Northern Taiwan) at K = 5

STRUCTURE analyses conducted separately for each island revealed weaker signals of within-island genetic structure. For the Ishigaki cluster (789 SNPs, 234 unlinked loci), ΔK values showed moderate support for $K = 5$ ($\Delta K = 3.115$; mean LnP(K) = -4096.0 ± 92.2; Fig. S2-A); however, individual assignment probabilities showed extensive admixture and did not indicate clear genetic subdivision within the island (Fig. S2-B). Similarly, for the Iriomote cluster (986 SNPs, 222 unlinked loci), ΔK strongly supported $K = 4$ ($\Delta K = 10.863$; mean LnP(K) = -2694.3 ± 77.9; Fig. S3-A), but STRUCTURE bar plots showed high admixture among inferred clusters, with no clear geographic or population-level differentiation within Iriomote Island (Fig. S3-B).

In PCA, PC1, PC2, and PC3 contributed 28.6%, 14.6%, and 4.1%, respectively. PC1 and PC2 were divided into the Ishigaki, Iriomote, and Taiwanese clusters, while PC1 and PC3 were divided into the Northern Taiwanese and Central Taiwanese clusters (Fig. 5).

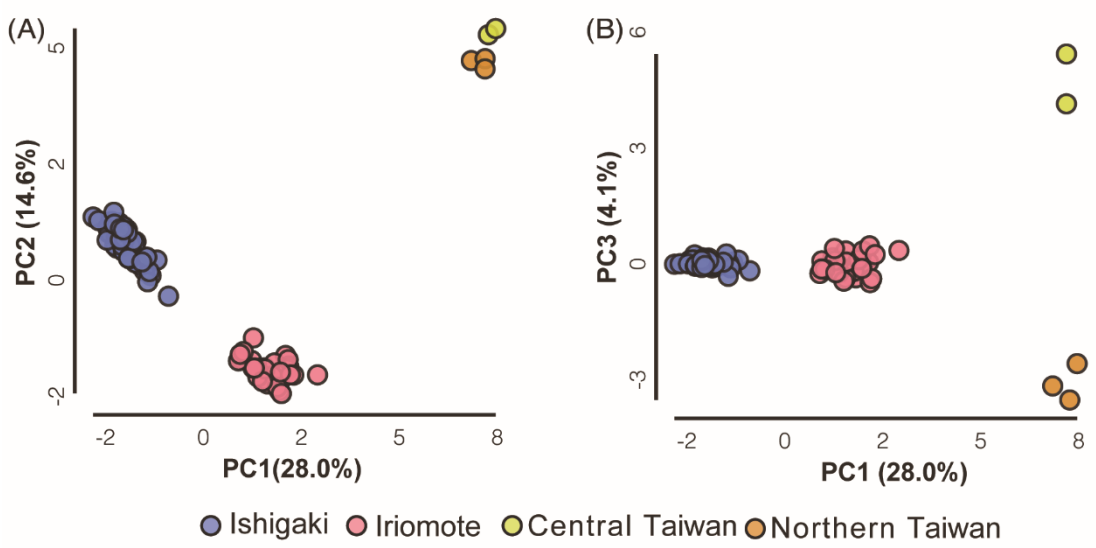

Fig. 5. Results of principal component analysis of *K. eiffingeri* based on SNPs. The numbers in parentheses indicate the contribution ratio. (A) shows the results of PC1 vs. PC2, where the samples were divided into three groups (Ishigaki, Iriomote, Taiwan clusters). (B) shows the results of PC1 vs. PC3, in which the individuals from Taiwan were divided into two populations (the Central and the Northern Taiwan).

Demographic inference using dadi

Demographic history between the Ishigaki and Iriomote clusters was inferred using dadi by comparing four alternative demographic models: Strict Isolation (SI), Isolation with Migration (IM), Ancient Migration (AM), and Secondary Contact (SC). Among these models, the SC model provided the best fit to the data (log-likelihood = -443.69, AIC = 899.38), whereas the IM, AM, and SI models received substantially less support (ΔAIC = 108.72, 141.25, and 396.14, respectively). Under the SC model, the Ishigaki and Iriomote clusters were inferred to have diverged, remained isolated for an extended period (Tiso = 0.889), and subsequently experienced recent secondary contact (Tsc = 0.015). Relative effective population size estimates indicated that the Iriomote cluster (ν_2 = 6.46) experienced a greater expansion than the Ishigaki cluster (ν_1 = 1.05). Migration was inferred to occur in both directions following secondary contact, with a higher migration rate from the Iriomote cluster to the Ishigaki cluster (m_{12} = 6.29) than in the opposite direction (m_{12} = 0.85) (Fig. 2).

Assuming that the previously estimated mtDNA divergence time between the two island clusters (1.41 Ma, 95% CI: 0.81–2.02 Ma; Kamimura et al. 2025) corresponds to Tiso (= 0.889), the estimated timing of secondary contact (Tsc = 0.015) corresponds to approximately 23.8 ka (approximately 13.7–34.1 ka based on the 95% confidence interval of the mtDNA estimate).

DISCUSSION

Evolutionary History Revealed by Genome-wide SNP Data

The results of STRUCTURE analysis, principal component analysis (PCA), and phylogenetic reconstruction based on MIG-seq data in this study were congruent with the previous mtDNA findings (Kamimura et al. 2025), consistently detecting four clusters of *Kurixalus eiffingeri* corresponding to Central Taiwan, Northern Taiwan, Iriomote, and Ishigaki (Fig. 3). This congruent pattern of genetic divergence observed in both mtDNA and nuclear DNA (nuDNA) suggests that gene flow among these clusters has been highly restricted over a long evolutionary timescale.

However, demographic inference using dadi suggested a more complex evolutionary history, supporting a secondary contact model between the Ishigaki and Iriomote clusters (Fig. 2). The timing of the second contact between the Ishigaki and Iriomote clusters was estimated at 23.8 ka (95% CI: 13.7–34.1 ka), falling within the period of the Last Glacial Maximum when a land bridge connected Ishigaki and Iriomote Islands. These results suggest that, although secondary contact during the Pleistocene land bridge formation resulted in gene flow between the Ishigaki and Iriomote clusters, the extent of gene flow was insufficient to erode their genetic distinctiveness.

The Filtering Effect of Pleistocene Land Bridges on Dispersal

Ishigaki Island and Iriomote Island are geographically close and were repeatedly connected by land bridge during Pleistocene glacial periods (Kizaki and Oshiro 1977 1980; Ujiie 1986; Kimura 1996; Lambeck and Chappell 2001; Bintanja et al. 2005; Bintanja and Roderik 2008; Fernández-Palacios et al. 2016). Our results and previous studies suggest that successful dispersal across the land bridge was strongly species-dependent, and that the land bridge has functioned as a filter bridge (Simpson 1940), allowing successful dispersal only for species with suitable ecological traits.

Previous phylogenetic studies based on mtDNA revealed that no clear genetic differentiation between Ishigaki and Iriomote clusters in several amphibian species (*e.g.*, *Odorrana supranarina*, *Buergeria choui,* and *Microhyla kuramotoi*) (Matsui et al. 2005; Tominaga et al. 2015; Tominaga et al. 2019), suggesting that sufficient gene flow via the Pleistocene land bridge prevented substantial genetic differentiation between the two island populations.

In contrast, *Odorrana utsunomiyaorum*, which also occurs on both islands, shows marked genetic divergence between the Ishigaki and Iriomote populations (Matsui et al. 2005). Because *O. utsunomiyaorum* inhabits only mountainous areas with running streams, Matsui et al. (2005) suggested that the land bridge connecting Ishigaki and Iriomote Islands lacked suitable freshwater habitats, which may have limited opportunities for dispersal and genetic exchange between the two island populations.

The present results indicate that, although secondary contact between the two island clusters of *K. eiffingeri* occurred via the Pleistocene land bridge and resulted in limited gene flow, the extent of gene flow was insufficient to erode their genetic distinctiveness. *K. eiffingeri* is closely associated with forest habitats and breeds in arboreal water bodies, such as water-filled tree cavities and bamboo internodes (Ueda 1986; Matsui 2021). If forest vegetation and suitable breeding sites were scarce on the exposed Sekisei Lagoon during glacial periods, opportunities for successful dispersal and establishment across the land bridge would have been greatly reduced, thus limiting gene flow between the two island clusters.

In contrast to interisland differentiation, the absence of substantial genetic substructures within each island cluster (Fig. S2-B, Fig. S3-B) indicates that gene flow occurs readily within islands, likely facilitated by continuous forest habitats. *K. eiffingeri* appears to be constrained by its dependence on forest habitats and arboreal breeding sites. Nevertheless, the lack of genetic structure within each island suggests that these habitat requirements have not substantially restricted dispersal among forest patches within islands, where habitat connectivity has likely been maintained over evolutionary timescales.

Alternatively, a hybrid zone may have formed between the two clusters following secondary contact, while gene flow between them remained limited (Barton and Hewitt 1985 1989). Hybrid zones may remain geographically stable when dispersal is limited by ecological conditions and reduced population density in the contact region (Johannesson et al. 2020). If suitable habitats for *K. eiffingeri* were limited and population densities were low on the land bridge, hybrid zone may have been trapped within the land bridge, preventing gene flow between the islands. If so, this scenario would require at least some degree of reproductive isolation between the two clusters, a possibility that should be examined through future crossing experiments.

Future Perspectives on Genetic Structure in Taiwan

Although the discussion above has focused on the Yaeyama clusters, the pronounced genetic differentiation observed within Taiwan also raises important biogeographical questions. In particular, the historical and contemporary relationships between the Northern and Central Taiwan clusters remain unresolved because the sampling sites included in this study were geographically distant from one another. Resolving this issue will require more extensive and spatially dense sampling across the putative contact zone, together with genome-wide data and high-resolution population genomic analyses, to determine whether the observed genetic structure reflects true evolutionary lineages or continuous geographic variation.

CONCLUSIONS

Our genome-wide SNP analyses demonstrate that the evolutionary history and genetic differentiation in *Kurixalus eiffingeri* cannot be explained solely by a simple divergence model. Instead, demographic inference supports a scenario of divergence followed by secondary contact with limited gene flow, indicating that genetic distinctiveness between the two clusters has been maintained despite secondary contact. Lineage divergence appears to have been shaped by the combined effects of geological history, habitat availability, and species-specific ecological characteristics, highlighting the importance of ecological barriers, even where a temporary land bridge existed. These findings provide new insights into the processes driving diversification in continental island systems and underscore the need to consider both geological and ecological factors when interpreting phylogeographic patterns in island taxa. Future studies integrating broader geographic sampling, demographic modelling, paleoecological reconstruction, and comparisons of ecological and behavioral traits, such as advertisement calls among island populations, will further clarify the mechanisms maintaining lineage divergence and the evolutionary history of the Ryukyu Archipelago biota.

Acknowledgments: We thank N. Sakashita for helping with the field work in this study. This work was partially supported by the University of the Ryukyus Research Project Promotion Grant (Strategic Research Grant) to M. Izawa (principal investigator). This research also received partial support from MEXT KAKENHI, Grant Number 21H05181, to K. Araya (principal investigator). The first author (RK) expresses his gratitude to M. Toda and T. Denda for their valuable guidance and advice throughout this study. The first author (RK) also sincerely thanks N. Nagata and M. Hiruta for their guidance on SNP analyses. We are also grateful the two anonymous reviewers and S. M. Lin for suggestions that improved the manuscript.

Authors' contributions: RK: Writing – original draft, Writing – review & editing, Investigation, Formal analysis, Conceptualization. SS: Investigation. CSW: Writing – review & editing, Investigation. YHC: Writing – review & editing, Investigation. MM: Writing – review & editing, Investigation. NY: Writing – review & editing, Investigation, Formal analysis. AT: Writing – review & editing, Investigation, Funding acquisition, Supervision, Project administration, Conceptualization.

Competing interests: The authors declare that they have no known competing financial interests or personal relationships that could have appeared to influence the work reported in this paper.

Availability of data and materials: The analysis files (HDF5 format) used in this study have been deposited in figshare (10.6084/m9.figshare.31368484). The filtered VCF files have also been deposited in the same repository.

Consent for publication: All the authors consent to the publication of this manuscript.

Ethics approval consent to participate: Sampling was conducted with the approval of the Animal Experiment Committee of the University of the Ryukyus (Permit No. A2021054).

REFERENCES

Barton NH, Hewitt GM. 1985. Analysis of hybrid zones. Annu Rev Ecol Evol Syst **16:**113–148. doi:10.1146/annurev.es.16.110185.000553.

Barton NH, Hewitt GM. 1989. Adaptation, speciation and hybrid zones. Nature **341:**497–503. doi:10.1038/341497a0.

Bintanja R, Roderik SW, van de Wal, Oerlemans J. 2005. Modelled atmospheric temperatures

and global sea levels over the past million years. Nature **437:**125–128. doi:10.1038/nature03975.

Bintanja R, Roderik SW, van de Wal. 2008. North American ice-sheet dynamics and the onset of 100,000-year glacial cycles. Nature **454:**869–872. doi:10.1038/nature07158.

Brandley MC, Wang Y, Guo X, Montes de Oca AN, Feria-Ortiz M et al. 2011. Accommodating heterogenous rates of evolution in molecular divergence dating methods: an example using intercontinental dispersal of *Plestiodon* (Eumeces) lizards. Syst Biol **60:**3–15. doi:10.1093/sysbio/syq045.

De Queiroz A. 2005. The resurrection of oceanic dispersal in historical biogeography. Trends Ecol Evol **20:**68–73. doi:10.1016/j.tree.2004.11.006.

Dufresnes C, Nicieza AG, Litvinchuk SN, Rodrigues N, Jeffries DL et al. 2020. Are glacial refugia hotspots of speciation and cytonuclear discordances? Answers from the genomic phylogeography of Spanish common frogs. Mol Ecol **29:**986–1000. doi:10.1111/mec.15368.

Eaton DA, Overcast I. 2020. ipyrad: Interactive assembly and analysis of RADseq datasets. Bioinformatics **36:**2592–2594. doi:10.1093/bioinformatics/btz966.

Evanno G, Regnaut S, Goudet J. 2005. Detecting the number of clusters of individuals using the software STRUCTURE: a simulation study. Mol Ecol **14:**2611–2620. doi:10.1111/j.1365-294x.2005.02553.x.

Fernández-Palacios JM, Rijsdijk KF, Norder SJ, Otto R, de Nascimento L et al. 2016. Towards a glacial-sensitive model of island biogeography. Glob Ecol Biogeogr **25:**817–830. doi:10.1111/geb.12320.

Ge D, Feijó A, Wen Z, Lissovsky A, Zhang D et al. 2022. Ancient introgression underlying the unusual mito-nuclear discordance and coat phenotypic variation in the Moupin pika. Divers Distrib **28:**2593–2609. doi:10.1111/ddi.13479.

Gutenkunst RN, Hernandez RD, Williamson SH, Bustamante CD. 2009. Inferring the joint demographic history of multiple populations from multidimensional SNP frequency data.

PLoS Genetics **5:**e1000695. doi:10.1371/journal.pgen.1000695.

Horoiwa M, Mandagi IF, Sutra N, Montenegro J, Tantu FY et al. 2021. Mitochondrial introgression by ancient admixture between two distant lacustrine fishes in Sulawesi Island. PLoS ONE **16:**e0245316. doi:10.1371/journal.pone.0245316.

Jakobsson M, Rosenberg NA. 2007. CLUMPP: a cluster matching and permutation program for dealing with label switching and multimodality in analysis of population structure. Bioinformatics **23:**1801–1806. doi:10.1093/bioinformatics/btm233.

Johannesson K, Le Moan A, Perini S, André C. 2020. A Darwinian laboratory of multiple contact zones. Trends Ecol Evol **35:**1021–1036. doi:10.1016/j.tree.2020.07.015.

Kaito T, Toda M. 2016. The biogeographical history of Asian keelback snakes of the genus *Hebius* (Squamata: Colubridae: Natricinae) in the Ryukyu Archipelago, Japan. Biol J Linn Soc **118:**187–199. doi:10.1111/bij.12726.

Kamimura R, Sakihama S, Wu CS, Chen YH, Matsui M et al. 2025. Speciation on the continent in the Miocene? Multiple overseas dispersal to the island? –Reexamination of diversification process of *Kurixalus eiffingeri* (Boettger, 1895) (Amphibia: Rhacophoridae)–. Zool Anz **316:**298–308. doi:10.1016/j.jcz.2025.04.010.

Kanke E, Suzuki K, Sekiné K, Suzuki T, Hatta K, Yang MM, Tojo K. 2021. Unexpected population genetic structure in two closely related euphaeid damselflies from the Yaeyama and Taiwan Islands (Odonata: *Euphaeidae*). Biol J Linn Soc 134:214–228. doi:10.1093/biolinnean/blab061.

Kato S, Arakaki S, Nagano AJ, Kikuchi K, Hirase S. 2024. Genomic landscape of introgression from the ghost lineage in a gobiid fish uncovers the generality of forces shaping hybrid genomes. Mol Ecol **33:**e17216. doi:10.1111/mec.17216.

Kimura M, 1996. Quaternary paleogeography of the Ryukyu Arc. J Geogr **105:**259–285. (in Japanese).

Kizaki K, Oshiro I. 1977. Paleogeography of the Ryukyu Islands. Marine Sci Monthly **9:**542–549. (in Japanese)

Kizaki K, Oshiro I. 1980. The origin of the Ryukyu Islands. *In*: Kizaki K ed. Natural history of the Ryukyus. Tokyo: Tsukiji shokan, pp. 8–37 (in Japanese)

Kozlov AM, Darriba D, Flouri T, Morel B, Stamatakis A. 2019. RAxML-NG: a fast, scalable and user-friendly tool for maximum likelihood phylogenetic inference. Bioinformatics **35:**4453–4455. doi:10.1093/bioinformatics/btz305.

Kvie KS, Hogner S, Aarvik L, Lifjeld JT, Johnsen A. 2013. Deep sympatric mt DNA divergence in the autumnal moth (*Epirrita autumnata*). Ecol Evol **3:**126–144. doi:10.1002/ece3.434.

Lambeck K, Chappell J. 2001. Sea level change through the last glacial cycle. Science **292:**679–686. doi:10.1126/science.1059549.

Lomolino MV, Riddle BR, Brown JH. 2006. Biogeography. 3rd Edition, Sinauer Associates, Inc., Sunderland.

MacArthur RH, Wilson EO. 1963. An equilibrium theory of insular zoogeography. Evolution **17:**373–387. doi:10.1111/j.1558-5646.1963.tb03295.x.

Marshall TL, Chambers EA, Matz MV, Hillis DM. 2021. How mitonuclear discordance and geographic variation have confounded species boundaries in a widely studied snake. Mol Phylogenet Evol **162:**107194. doi:10.1016/j.ympev.2021.107194.

Matsui M. 2021. *In*: Kurixalus Ye, Fei et Dubois in Fei, 1999. Herpetological Society of Japan (Ed) Amphibians and Reptiles of Japan. Sunrise Publishing, Hikone, Japan, pp. 78–79 (in Japanese)

Matsui M, Shimada T, Ota H, Tanaka-Ueno T. 2005. Multiple invasions of the Ryukyu Archipelago by Oriental frogs of the subgenus *Odorrana* with phylogenetic reassessment of the related subgenera of the genus *Rana*. Mol Phylogenet Evol **37:**733–742. doi:10.1016/j.ympev.2005.04.030.

Motokawa J. 2000. Biogeography of living mammals in the Ryukyu Islands. Tropics **10:**63–71.

Ota H. 1998. Geographic patterns of endemism and speciation in amphibians and reptiles of the Ryukyu Archipelago, Japan, with special reference to their paleogeographical implications. Res Popul Ecol **40:**189–204. doi:10.1007/bf02763404.

Pritchard JK, Stephens M, Rosenberg NA, Donnelly P. 2000. Association mapping in structured populations. Am J Hum Genet **67:**170–181. doi:10.1086/302959.

Ryan WBF, Carbotte SM, Coplan J, O'Hara S, Melkonian A et al. 2009. Geochem Geophys Geosyst **10:**Q03014. doi:10.1029/2008GC002332.

Shead TM. 2014. toyplot (Version 00) [Computer software]. Available at: https://www.osti.gov//servlets/purl/1335046.

Shimada T, Matsui M, Ogata M, Miura I, Tange M et al. 2022. Genetic and morphological variation analyses of *Glandirana rugosa* with description of a new species (Anura, Ranidae). Zootaxa **5174:**25–45. doi:10.11646/zootaxa.5174.1.2.

Simpson GG. 1940. Mammals and land bridge. J Wash Acad Sci **30:**137–163.

Stelbrink B, Albrecht C, Hall R, von Rintelen T. 2012. The biogeography of Sulawesi revisited: is there evidence for a vicariant origin of taxa on Wallace's "anomalous island"?. Evolution: International Journal of Organic Evolution **66:**2252–2271. doi:10.1111/j.1558-5646.2012.01588.x.

Su YC, Brown RM, Chang YH, Lin CP, Tso IM. 2016. Did a Miocene–Pliocene island isolation sequence structure diversification of funnel web spiders in the Taiwan-Ryukyu Archipelago?. J Biogeogr **43:**991–1003. doi:10.1111/jbi.12674.

Suyama Y, Matsuki Y. 2015. MIG-seq: an effective PCR-based method for genome-wide single-nucleotide polymorphism genotyping using the next-generation sequencing platform. Sci Rep **5:**1–12. doi:10.1038/srep16963

Tavaré S. 1986. Some probabilistic and statistical problems in the analysis of DNA sequences. Lect Math Life Sci **17:**57–86.

Toews DP, Brelsford A. 2012. The biogeography of mitochondrial and nuclear discordance in animals. Mol Ecol **21:**3907–3930. doi:10.1111/j.1365-294x.2012.05664.x.

Tominaga A, Matsui M, Eto K, Ota H. 2015. Phylogeny and differentiation of wide-ranging Ryukyu Kajika frog *Buergeria japonica* (Amphibia: Rhacophoridae): geographic genetic pattern not simply explained by vicariance through strait formation. Zool Sci **32:**240–247.

doi:10.2108/zs140227.

Tominaga A, Matsui M, Shimoji N, Khonsue W, Wu CS et al. 2019. Relict distribution of *Microhyla* (Amphibia: Microhylidae) in the Ryukyu Archipelago: High diversity in East Asia maintained by insularization. Zool Scr **48:**440–453. doi:10.1111/zsc.12361

Tominaga A, Yoshikawa N, Matsui M, Nagata N, Sato Y. 2022. The emergence of a cryptic lineage and cytonuclear discordance through past hybridization in the Japanese fire-bellied newt, *Cynops pyrrhogaster* (Amphibia: Urodela). Biol J Linn Soc **137:**651–666. doi:10.1093/biolinnean/blac120.

Tran LN, Sun CK, Struck TJ, Sajan M, Gutenkunst RN. 2024. Computationally efficient demographic history inference from allele frequencies with supervised machine learning. Mol Biol Evol **41:**msae077. doi:10.1093/molbev/msae077.

Ueda H. 1986. Reproduction of *Chirixalus eiffingeri* (Boettger). Sci Rep Lab Amphibian Biol, Hiroshima Univ **8:**109–116.

Ujiie H. 1986. The sea-bed of the Ryukyu Islands Arc. Sinseitosho-shuppan, Naha. (in Japanese)

Wilson EO, MacArthur RH. 1967. The theory of island biogeography (Vol. 1). Princeton, NJ: Princeton University Press.

Witt CC, Maliakal-Witt S. 2007. Why are diversity and endemism linked on islands?. Ecography **30:**331–333. doi:10.1111/j.2007.0906-7590.04837.x.

Yoder AD, Nowak MD. 2006. Has vicariance or dispersal been the predominant biogeographic force in Madagascar? Only time will tell. Annu Rev Ecol Evol Syst **37:**405–431. doi:10.1146/annurev.ecolsys.37.091305.110239.

Zeng J, Wang JS, Yu GH, Du LN. 2021. A new species of *Kurixalus* (Anura, Rhacophoridae) from Guizhou, China. Zool Res **42:**227. doi:10.24272/j.issn.2095-8137.2020.311.

Supplementary materials

Fig S1. (A) Bayesian clustering results from STRUCTURE analysis implemented in ipyrad. The red line shows the mean log probability of the data [LnP(K)], and the blue line shows ΔK calculated according to Evanno et al. for K = 2–10. The maximum ΔK was detected at K = 3. (B) Results of STRUCTURE analysis indicating admixture rate in each individual based on SNPs in Ishigaki Island, Iriomote Island, and Taiwan (K = 2–5). (download)

Fig S2. (A) Bayesian clustering results from STRUCTURE analysis implemented in ipyrad. The red line shows the mean log probability of the data [LnP(K)], and the blue line shows ΔK calculated according to Evanno et al. for K = 2–8. The maximum ΔK was detected at K = 5. (B) Results of STRUCTURE analysis indicating admixture rate in each individual based on SNPs in Ishigaki Island (K = 4–6). (download)

Fig S3. (A) Bayesian clustering results from STRUCTURE analysis implemented in ipyrad. The red line shows the mean log probability of the data [LnP(K)], and the blue line shows ΔK calculated according to Evanno et al. for K = 2–8. The maximum ΔK was detected at K = 4. (B) Results of STRUCTURE analysis indicating admixture rate in each individual based on SNPs in Iriomote Island (K = 3–5). (download)